

Reconstruction of the Extended Gauge Structure from Z' Observables at Future Colliders

F. DEL AGUILA

*Departamento de Física Teórica y del Cosmos, Universidad de Granada
Granada, 18071, Spain*

M. CVETIČ and P. LANGACKER

*Department of Physics, University of Pennsylvania
Philadelphia, PA 19104-6396*

(January 1995)

Abstract

The discovery of a new neutral gauge boson Z' with a mass in the TeV region would allow for determination of gauge couplings of the Z' to ordinary quarks and leptons in a model independent way. We show that these couplings in turn would allow us to determine the nature of the extended gauge structure. As a prime example we study the E_6 group. In this case two discrete constraints on experimentally determined couplings have to be satisfied. If so, the couplings would then uniquely determine the two parameters, $\tan \beta$ and δ , which fully specify the nature of the Z' within E_6 . If the Z' is part of the E_6 gauge structure, then for $M_{Z'} = 1$ TeV $\tan \beta$ and δ could be determined to around 10% at the future colliders. The NLC provides a unique determination of the two constraints as well as of $\tan \beta$ and δ , though with slightly larger error bars than at the LHC. On the other hand, since the LHC primarily determines three out of four normalized couplings, it provides weaker constraints for the underlying gauge structure.

I. INTRODUCTION

New neutral (Z') and charged (W') gauge bosons are a generic prediction of theories beyond the standard model. If their mass turns out to be in the TeV region future hadron colliders (the Large Hadron Collider (LHC) at CERN) as well as e^+e^- colliders (the New Large Collider (NLC)) would provide an ideal environment for their discovery as well as for further testing of their properties.

In recent years it has been demonstrated that for $M_{Z',W'} \sim 1$ TeV a diagnostic study of heavy gauge bosons is possible at the LHC (integrated luminosity $\mathcal{L}_{int} = 100 \text{ fb}^{-1}$, center of mass energy $\sqrt{s} = 14$ TeV) [1,2]¹ as well as at the NLC ($\mathcal{L}_{int} = 20 \text{ fb}^{-1}$, $\sqrt{s} = 500$ GeV) [4]. Both machines turn out to have complementary diagnostic power for Z' physics [5].

For $M_{Z'} \leq 1 - 2$ TeV the future colliders allow for model independent determination of gauge couplings to quarks and leptons. The analysis assumes family universality; $[Q', T_i] = 0$, where Q' is the $U(1)'$ charge and T_i are the generators of $SU(2)_L$; and that $Z - Z'$ mixing is negligible. The LHC can probe the absolute magnitude of the overall strength of the new interaction g_2 , as well as the magnitude of (primarily) three out of four normalized gauge couplings. On the other hand, the NLC with longitudinal electron beam polarization and heavy flavor tagging available is sensitive to the ratio of $g_2^2/M_{Z'}^2$, and four normalized gauge couplings. The latter can also be determined in terms of normalized couplings probed directly at the LHC; the error bars are typically smaller by a factor of ~ 2 than those at the NLC [5], but there is a few-fold ambiguity. Thus, the LHC and the NLC are complementary and together have the potential to uniquely determine the couplings with small error-bars. For $M_{Z'} \sim 1$ TeV the error bars are in the 10%-20% region.

In this note we point out that a model independent determination of gauge couplings in turn provides a tool to learn more about the nature of the extended gauge structure. In particular, one would be able to gain information about the underlying gauge group and subsequently probe the type of symmetry breaking associated with the new heavy gauge boson.

To illustrate the method we study as a prime example the Cartan subalgebra of the E_6 gauge group, which provides a general enough framework for grand unified symmetry with canonical embedding of electric charge and simple cancellation of anomalies. In addition, it is motivated by string theory. E_6 imposes two discrete constraints on the Z' gauge couplings. Provided these are satisfied by the measured couplings, one can further determine the two parameters $\tan\beta$ and δ . These two parameters, together with the overall strength of the new gauge couplings g_2 , contain the information brought by the new interaction concerning the pattern of symmetry breaking, possible intermediate mass scales, and renormalization effects above the Z' . This window to higher scales, as in the case of the weak angle, is not sufficient to fix the full theory at the Planck scale, but it should allow for constraining possible unification schemes, excluding many possibilities. See, for instance, Refs. [6,7] for a discussion of the predictions for the new parameters of extended models from the heterotic string.

¹Production rates have recently been recalculated in Ref. [3].

In Section II we spell out the formalism and parameterization of the Z' interaction with the corresponding quark and lepton neutral currents. In Section III we recapitulate the results for the model independent determination of gauge couplings. In Section IV we illustrate how such couplings allow for a determination of the underlying gauge symmetry and subsequently for determination of the symmetry breaking pattern with a particular gauge structure. Conclusions are given in Section V.

II. FORMALISM

The coupling of an additional neutral gauge boson Z' and the neutral standard model bosons W_3, B to ordinary fermions are parameterized in the neutral current Lagrangian as [7,8]:

$$-\mathcal{L}_{NC} = \bar{\psi}_k \gamma^\mu [T_{3k} g W_{3\mu} + Y_k g_1 B_\mu + (Q'_k g_2 + Y_k g_{12}) Z'_\mu] \psi_k, \quad (1)$$

where T_3 and Y are the standard model isospin and hypercharge charges, respectively, and Q' is the charge of the extra $U(1)'$. A sum over all the quarks and leptons ψ_k is implied. This Lagrangian describes the general coupling of a new gauge boson Z' with charge Q' which commutes with the $SU(2)_L$ generators T_i , *i.e.*, $[Q', T_i] = 0$. This is the case for all of the extended gauge structures for which the generator of the $U(1)'$ associated with Z' lies in its Cartan subalgebra. In the following we also assume family universality and neglect $Z - Z'$ mixing, as indicated by present bounds [9] and the expected accuracy at future colliders.

The Z' couplings are specified by the (normalized) charges Q'_k and the overall strength g_2 , as well as by g_{12} , which is the coupling of Z' to the weak hypercharge. Thus, the neutral current Lagrangian of the ordinary fermions, which includes an additional gauge boson, is specified by five charges $g_2 Q'_k$ and the relative strength of the Z' gauge coupling to the hypercharge Y and the Q' currents, $\delta \equiv g_{12}/g_2$. The charges Q'_k are characteristic of the underlying extended gauge structure. Q'_k charges for typical models based on $SO(10)$ and E_6 grand unified symmetries are given in Table I. The $SO(10)$ symmetry includes the general *left-right* symmetric models with [7]

$$g_2 = \frac{e}{c_W} \sqrt{\frac{2}{5} \frac{\rho^2 + 1}{\rho}}, \quad \delta = \frac{g_{12}}{g_2} = \sqrt{\frac{1}{6} \frac{3\rho^2 - 2}{\rho^2 + 1}}, \quad \rho = \sqrt{\kappa^2 \cot^2 \theta_W - 1}, \quad (2)$$

where $\kappa = \frac{g_R}{g_L}$ is the ratio of the gauge couplings $g_{L,R}$ for $SU(2)_{L,R}$, respectively. In general, $\kappa > \frac{s_W}{c_W}$ [10]. Here $c_W \equiv \cos \theta_W$ and $s_W \equiv \sin \theta_W$ where θ_W is the weak angle.

For a particular extended gauge symmetry the charges Q'_k are fixed numbers which usually satisfy specific constraints. For $SO(10)$ the Q'_k satisfy the four conditions:

$$Q'_{e_L^c} = Q'_{u_L^c} = Q'_{q_L}, \quad Q'_{\ell_L} = Q'_{d_L^c}, \quad Q'_{d_L^c} = -3 Q'_{q_L}, \quad (3)$$

whereas for E_6 only the first three are satisfied in general.

The gauge couplings, $g, g_{1,2,12}$, specify the overall strength of the interactions. They are fixed at the large scale, where the full underlying gauge structure is present, *e.g.*, in string theory the gauge couplings of all the group factors are related at the string compactification

TABLE I. Isospin T_3 , hypercharge Y , and Q' charges for ordinary quarks and leptons. Q_χ specifies the additional $SO(10)$ charge, whereas Q_ψ is the additional charge in the breaking of E_6 to $SO(10)$. Thus, $Q_\beta = Q_\chi \cos \beta + Q_\psi \sin \beta$ is the general E_6 charge. The charges $Q_{\chi,\psi,\eta}$ of the particular models correspond to Q_β with $\beta = 0, \frac{\pi}{2}, -\tan^{-1} \sqrt{\frac{5}{3}}$, respectively.

Fermions	T_3	$\sqrt{\frac{5}{3}}Y$	Q'	$2\sqrt{10}Q_\chi$	Q_β
$\begin{pmatrix} u \\ d \end{pmatrix}_L$	$\begin{pmatrix} \frac{1}{2} \\ -\frac{1}{2} \end{pmatrix}$	$\frac{1}{6}$	Q'_{qL}	-1	$-\frac{1}{2\sqrt{10}} \cos \beta + \frac{1}{2\sqrt{6}} \sin \beta$
u_L^c	0	$-\frac{2}{3}$	Q'_{uL^c}	-1	$-\frac{1}{2\sqrt{10}} \cos \beta + \frac{1}{2\sqrt{6}} \sin \beta$
d_L^c	0	$\frac{1}{3}$	Q'_{dL^c}	3	$\frac{3}{2\sqrt{10}} \cos \beta + \frac{1}{2\sqrt{6}} \sin \beta$
$\begin{pmatrix} \nu \\ e \end{pmatrix}_L$	$\begin{pmatrix} \frac{1}{2} \\ -\frac{1}{2} \end{pmatrix}$	$-\frac{1}{2}$	$Q'_{\ell L}$	3	$\frac{3}{2\sqrt{10}} \cos \beta + \frac{1}{2\sqrt{6}} \sin \beta$
e_L^c	0	1	Q'_{eL^c}	-1	$-\frac{1}{2\sqrt{10}} \cos \beta + \frac{1}{2\sqrt{6}} \sin \beta$

scale. However, these couplings are renormalized at low energies, where their values crucially depend on the matter content, the symmetry breaking pattern, and the threshold effects. In particular, g_{12} may vanish at the large scale, but it is in general non-zero at low energy. It allows for description of the *left-right* models (see Eq. (2)) within the $SO(10)$ symmetry. Introduction of g_{12} is also necessary for a complete parameterization of low energy models when only the extended gauge structure or its Cartan subalgebra, within which Q' lies, is known².

III. MODEL INDEPENDENT DETERMINATION OF Z' COUPLINGS AT THE LHC AND THE NLC

The NLC would be able to probe in a model independent way the following suitable combinations of normalized gauge couplings [5]:

$$P_V^\ell = \frac{\hat{g}_L^\ell + \hat{g}_R^\ell}{\hat{g}_L^\ell - \hat{g}_R^\ell}, \quad P_L^q = \frac{\hat{g}_L^q}{\hat{g}_L^\ell - \hat{g}_R^\ell}, \quad P_R^{u,d} = \frac{\hat{g}_R^{u,d}}{\hat{g}_L^q}, \quad (4)$$

as well as the ratio

$$\epsilon_A = (\hat{g}_L^\ell - \hat{g}_R^\ell)^2 \frac{g_2^2}{4\pi\alpha M_{Z'}^2 - s}. \quad (5)$$

²Without loss of generality the gauge coupling g_{21} , which parameterizes the strength of the B coupling to the neutral currents specified by Q' , can be set to zero. Gauge couplings of B and Z' to the neutral currents specified by T_3 vanish by gauge invariance [8].

Here \hat{g}_k are the normalized Z' couplings to ordinary fermions in Eq. (1), $\hat{g}_k = Q'_k + \delta Y_k$ (see Ref. [11] for conventions and notation). The values of these couplings within the general underlying E_6 gauge structure are given in Table II. In Table III we define typical models (χ, ψ, η, LR , and general LR models) in terms of the parameters β and δ and the overall Z' gauge coupling, expressed in terms of the electric charge e and the weak angle.

On the other hand in addition to the mass $M_{Z'}$ the LHC will probe [1] an overall strength g_2 of the Z' couplings as well as three normalized couplings γ_L^ℓ, \tilde{U} , and \tilde{D} , where:

$$\gamma_L^\ell = \frac{(\hat{g}_L^\ell)^2}{(\hat{g}_L^\ell)^2 + (\hat{g}_R^\ell)^2}, \quad \tilde{U} = \frac{(\hat{g}_R^u)^2}{(\hat{g}_L^q)^2}, \quad \tilde{D} = \frac{(\hat{g}_R^d)^2}{(\hat{g}_L^q)^2}. \quad (6)$$

A fourth coupling,

$$\gamma_L^q = \frac{(\hat{g}_L^q)^2}{(\hat{g}_L^\ell)^2 + (\hat{g}_R^\ell)^2} \quad (7)$$

could be determined, provided the Z' cross section into quark pairs could be measured with sufficient precision. Recent studies indicate [12,13] that this might be feasible. It turns out [12], however, that for $M_{Z'} \geq 1$ TeV and the typical models specified in Table III the Z' gauge couplings are too small to allow for determination of γ_L^q with sufficient precision at the LHC. Thus, in the analysis the determination of γ_L^q is not included.

The couplings (4), probed directly at the NLC, are determined with a few-fold ambiguity in terms of the couplings (6) and (7) probed directly at the LHC. Namely, couplings probed at the NLC (Eq. (4)) are related to the couplings probed at the LHC (Eq.(6)) in the following way:

$$\begin{aligned} P_V^\ell &= \frac{1 + 2\epsilon_\ell \gamma_L^\ell \frac{1}{2} (1 - \gamma_L^\ell)^{\frac{1}{2}}}{2\gamma_L^\ell - 1}, \\ P_L^q &= \frac{1}{2} \epsilon_q \gamma_L^q \frac{1}{2} \left\{ 1 + \left[\frac{1 + 2\epsilon_\ell \gamma_L^\ell \frac{1}{2} (1 - \gamma_L^\ell)^{\frac{1}{2}}}{2\gamma_L^\ell - 1} \right]^2 \right\}^{\frac{1}{2}}, \\ P_R^u &= \epsilon_u \tilde{U}^{\frac{1}{2}}, \\ P_R^d &= \epsilon_d \tilde{D}^{\frac{1}{2}}. \end{aligned} \quad (8)$$

where $\epsilon_\ell, \epsilon_q, \epsilon_u, \epsilon_d$ can take \pm values and give rise to a sixteen-fold sign ambiguity. The inability to probe γ_L^q directly implies that P_L^q is not probed either.

For typical models (within the E_6 gauge structure), and $M_{Z'} = 1$ TeV the values and expected statistical error bars for the three couplings (6) [1] and the four couplings (4) [5] are given in Table IV. The error bars at the LHC update the analysis of Ref. [1]; the updated numbers correspond to the lower c.m. energy (14 TeV) and the (more optimistic) assumption that the branching ratios include Z' decays into ordinary three family fermions only.

In the analysis only statistical errors for the observables are included and error correlations for the input parameters are neglected. Experimental cuts and detector acceptances are not included either. The results should thus be interpreted as a limit on how precisely the couplings can be determined for each model for the given c.m. energy and the integrated

TABLE II. Z' couplings to ordinary fermions for E_6 models ($\beta = 0$ corresponds to $SO(10)$ models). The corresponding right-handed couplings are $\hat{g}_R^\psi = -\hat{g}_L^{\psi^c}$.

\hat{g}_k	$Q'_k + \delta Y_k$
\hat{g}_L^q	$-\frac{1}{2\sqrt{10}} \cos \beta + \frac{1}{2\sqrt{6}} \sin \beta + \delta \frac{1}{6} \sqrt{\frac{3}{5}}$
$\hat{g}_L^{u^c}$	$-\frac{1}{2\sqrt{10}} \cos \beta + \frac{1}{2\sqrt{6}} \sin \beta - \delta \frac{2}{3} \sqrt{\frac{3}{5}}$
$\hat{g}_L^{d^c}$	$\frac{3}{2\sqrt{10}} \cos \beta + \frac{1}{2\sqrt{6}} \sin \beta + \delta \frac{1}{3} \sqrt{\frac{3}{5}}$
\hat{g}_L^ℓ	$\frac{3}{2\sqrt{10}} \cos \beta + \frac{1}{2\sqrt{6}} \sin \beta - \delta \frac{1}{2} \sqrt{\frac{3}{5}}$
$\hat{g}_L^{\ell^c}$	$-\frac{1}{2\sqrt{10}} \cos \beta + \frac{1}{2\sqrt{6}} \sin \beta + \delta \sqrt{\frac{3}{5}}$

TABLE III. Parameterization of typical Z' models within E_6 . The value of ρ specifies a general LR model.

Model	β	δ	g_2
χ	0	0	$\sqrt{\frac{5}{3}} \frac{e}{c_W}$
ψ	$\frac{\pi}{2}$	0	$\sqrt{\frac{5}{3}} \frac{e}{c_W}$
η	$-\tan^{-1} \sqrt{\frac{5}{3}}$	0	$\sqrt{\frac{5}{3}} \frac{e}{c_W}$
LR	0	0.615	$1.382 \frac{e}{c_W}$
general LR	0	$\sqrt{\frac{1}{6}} \frac{3\rho^2 - 2}{\rho^2 + 1}$	$\sqrt{\frac{2}{3}} \frac{\rho^2 + 1}{\rho} \frac{e}{c_W}$
β	β	0	$\sqrt{\frac{5}{3}} \frac{e}{c_W}$

TABLE IV. Values and statistical error bars for γ_L^ℓ , \tilde{U} , \tilde{D} at the LHC and for P_V^ℓ , P_L^q , P_R^u , P_R^d at the NLC for the χ , ψ , η , LR models, with $M_{Z'} = 1$ TeV. The error bars in parentheses are for the probes without polarization [5]. We do not include a possible determination of γ_L^q .

	χ	ψ	η	LR
P_V^ℓ	$2 \pm 0.08(0.26)$	$0 \pm 0.04(1.5)$	$-3 \pm 0.5(1.1)$	$-0.15 \pm 0.018(0.072)$
P_L^q	$-0.5 \pm 0.04(0.10)$	$0.5 \pm 0.10(0.2)$	$2 \pm 0.3(1.1)$	$-0.14 \pm 0.037(0.07)$
P_R^u	$-1 \pm 0.15(0.19)$	$-1 \pm 0.11(1.2)$	$-1 \pm 0.15(0.24)$	$-6.0 \pm 1.4(3.3)$
P_R^d	$3 \pm 0.24(0.51)$	$-1 \pm 0.21(2.8)$	$0.5 \pm 0.09(0.48)$	$8.0 \pm 1.9(4.1)$
γ_L^ℓ	0.9 ± 0.016	0.5 ± 0.02	0.2 ± 0.012	0.36 ± 0.007
\tilde{U}	1 ± 0.16	1 ± 0.14	1 ± 0.08	37 ± 6.6
\tilde{D}	9 ± 0.57	1 ± 0.22	0.25 ± 0.16	65 ± 11

luminosity of the NLC and the LHC. Realistic fits are expected to give larger uncertainties.

IV. RECONSTRUCTION OF THE EXTENDED GAUGE STRUCTURE

We now demonstrate how the model independent determination of the normalized couplings in Eq. (4) or Eq. (6) allows for the testing of a particular underlying symmetry structure and, subsequently, how such couplings further constrain the symmetry breaking pattern. We demonstrate the procedure for models based on E_6 gauge symmetry.

As the first step in establishing the underlying E_6 symmetry structure, the normalized couplings should be compatible with the discrete constraints on the couplings of the type (3), which, in terms of the \hat{g} couplings, are:

$$\begin{aligned}
 2\hat{g}_L^q + \hat{g}_R^u + \hat{g}_R^\ell &= 0, \\
 \hat{g}_L^q - \hat{g}_R^d - \hat{g}_L^\ell + \hat{g}_R^\ell &= 0, \\
 3\hat{g}_L^q + \hat{g}_L^\ell &= 0.
 \end{aligned}
 \tag{9}$$

Only the first two equalities hold for general E_6 models. The third holds in the special case of $SO(10)$. At the NLC these constraints, expressed in terms of (4), are of the form:

$$\begin{aligned}
 C_1 &\equiv 2P_L^q(2 + P_R^u) + P_V^\ell - 1 = 0, \\
 C_2 &\equiv P_L^q(1 - P_R^d) - 1 = 0, \\
 C_3 &\equiv 6P_L^q + P_V^\ell + 1 = 0.
 \end{aligned}
 \tag{10}$$

The underlying gauge structure is therefore determined by the above constraints; the symmetry group corresponds to $SO(10)$ if the measured normalized couplings are compatible with all three constraints (10), while the symmetry group is E_6 if the measured couplings are compatible with the first two only.

The next step is to address the nature of the symmetry breaking pattern within the underlying symmetry structure.

The normalized couplings probed at the NLC (see Eq. (4)) in turn determine $\tan\beta$ and δ , parameterizing the most general symmetry breaking pattern within the E_6 group (recall $\beta = 0$ corresponds to the $SO(10)$ group). β and δ can be expressed in terms of the normalized couplings by:

$$\begin{aligned} \tan\beta &= \sqrt{15} \frac{P_L^q(1 - P_R^u) + 1}{P_L^q(1 + 3P_R^u - 4P_R^d) - 1 + 2P_V^\ell}, \\ \frac{\delta}{\cos\beta} &= 2\sqrt{6} \frac{P_L^q(1 + P_R^u)}{P_L^q(1 + 3P_R^u - 4P_R^d) - 1 + 2P_V^\ell}. \end{aligned} \quad (11)$$

Determination of the symmetry breaking pattern within the underlying gauge structure can be thought as replacing the phenomenological variables in (4) by the four independent variables C_1, C_2, β, δ in (10) and (11). (C_3 is a function of C_1 and β .) β and δ are interpreted as determining the pattern of symmetry breaking within E_6 for $C_1 = C_2 = 0$ only.

- One can determine the parameters in (4) and their correlation matrix from the NLC probes, and from these determine C_1, C_2, β , and δ (*step one*). If C_1 and C_2 are compatible with zero, then one assumes $C_1 = C_2 = 0$ (*step two*), *i.e.*, one assumes E_6 to be the underlying symmetry. In this case only two normalized couplings in (4) are independent, thus in turn implying that β and δ can be determined with better precision.
- Equivalently, one can rewrite the NLC probes as functions of C_1, C_2, β, δ and fit them directly to experimental data (*step one*). If C_1 and C_2 are compatible with zero, then one can fix them to be zero (*step two*), *i.e.*, one is assuming E_6 as the underlying symmetry, and then fit β and δ with higher precision.

We will use the second approach in our numerical examples below.

Before proceeding with the numerical analysis, we will introduce new convenient combinations of couplings, which in the case of E_6 symmetry are set to zero. The choice of variables C_1, C_2, β , and δ is suggested by the E_6 parameterization of charges. There is an equivalent choice of parameters:

$$S_1 = C_2, \quad S_2 = 2(2 + P_R^u) + (1 - P_R^d)(P_V^\ell - 1), \quad \beta, \quad \delta. \quad (12)$$

S_2 is a linear combination of C_1 and C_2 , which does not depend on P_L^q . Thus, $C_1 = C_2 = 0$ if and only if $S_1 = S_2 = 0$, *i.e.*, the latter set of constraints uniquely fix E_6 as the underlying symmetry as well. In the following we shall use variables (12) S_1, S_2, β , and δ , because they are better adapted to the analogous analysis at the LHC, and thus allow for an easy comparison of the NLC and the LHC potentials.

The analogous analysis at LHC requires one to rewrite (10), (11), (12) in terms of (6) and (7). This can be done using the relation (8). The sign ambiguity due to different sign assignments for $\epsilon_\ell, \epsilon_q, \epsilon_u$, and ϵ_d give rise to a sixteen-fold sign ambiguity due to the fact that at the LHC only the magnitude of the corresponding couplings is determined. In general,

TABLE V. Values and 1σ statistical error bars for S_1, S_2, β, δ , and ϵ_A at the NLC for the typical models. $M_{Z'} = 1$ TeV. The error bars in parentheses are determined by setting $S_1 = S_2 = 0$.

	χ	ψ	η	LR
S_1	0 ± 0.074	0 ± 0.18	0 ± 0.22	0 ± 0.074
S_2	0 ± 0.45	0 ± 0.37	0 ± 0.51	0 ± 0.76
β	$0 \pm 0.028(0.028)$	$1.57 \pm 0.043(0.027)$	$-0.912 \pm 0.038(0.028)$	$0 \pm 0.058(0.047)$
δ	$0 \pm 0.038(0.015)$	$0 \pm 0.035(0.014)$	$0 \pm 0.059(0.019)$	$0.615 \pm 0.032(0.008)$
ϵ_A	$0.071 \pm 0.005(0.005)$	$0.121 \pm 0.017(0.010)$	$0.012 \pm 0.003(0.003)$	$0.255 \pm 0.016(0.009)$

$C_1 = C_2 = 0$ ($S_1 = S_2 = 0$) can be satisfied only for a specific choice of the corresponding signs.³

A. Determination of the symmetry breaking structure at the NLC

As stated above we fit the expected NLC observables for S_1, S_2, β, δ and ϵ_A . In Table V the values and 1σ uncertainties for these quantities are given for the models specified in Table III and $M_{Z'} = 1$ TeV. The parameters β and δ can be determined with uncertainties between 0.02 and 0.06 for a large class of typical models. The large uncertainties for the η model are primarily due to the small value of ϵ_A . In Figure 1 we plot the 90% confidence level ($\Delta\chi^2 = 4.6$) contours (dashed lines) for two constraints (S_1 and S_2 as defined in (12)) for the models specified in Table III and $M_{Z'} = 1$ TeV. For the η model the uncertainties are slightly too large to allow for the corresponding 90% confidence level plot. In Figure 2 (dashed lines) we plot the 90% confidence level ($\Delta\chi^2 = 4.6$) contours in the β vs. δ plane for the typical models and $M_{Z'} = 1$ TeV.

As a second step we fix S_1, S_2 to zero, fitting the values of β, δ and ϵ_A . Clearly, the uncertainties are reduced. In Table V the corresponding 1σ uncertainties are given in parentheses. In this case even the parameters of the η model can be determined with a sufficient accuracy. The uncertainties are now reduced by a factor of 1 to 4 compared to the step one analysis. In Figure 2 the 90% confidence level ($\Delta\chi^2 = 4.6$) contours in the β vs. δ are plotted with solid lines.

Provided the mass $M_{Z'}$ is known by the time the NLC is turned on, the determination of the ϵ_A parameter would yield additional useful information on the overall strength g_2 and thus on the symmetry breaking patterns [14].

³Note, however, that for special values of δ and/or β parameters a few-fold sign ambiguity is not removed.

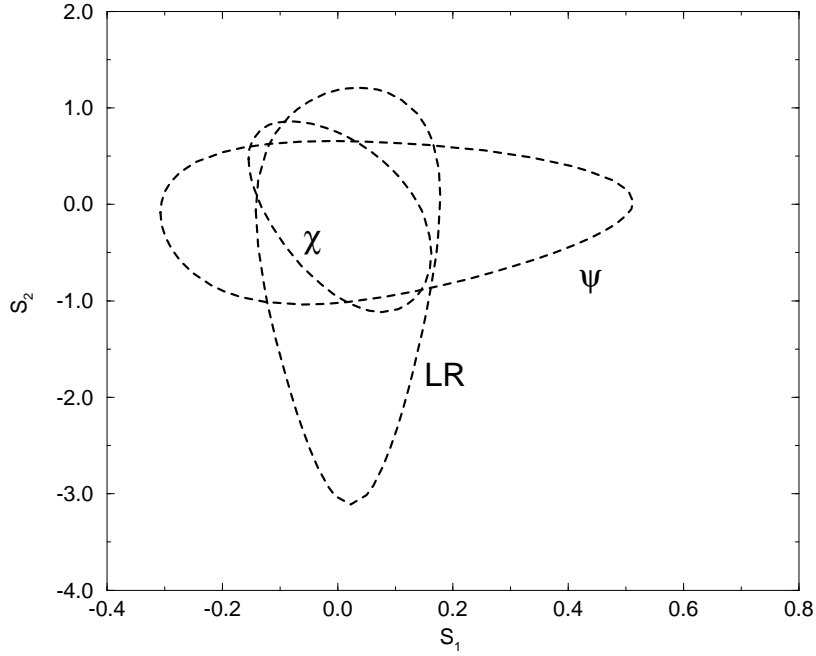


FIG. 1. 90% confidence level ($\Delta\chi^2 = 4.6$) contours for S_1 vs. S_2 (constraints defined in Eq. (12) for the typical models at the NLC. $M_{Z'} = 1$ TeV. Only statistical error bars for the probes are used.

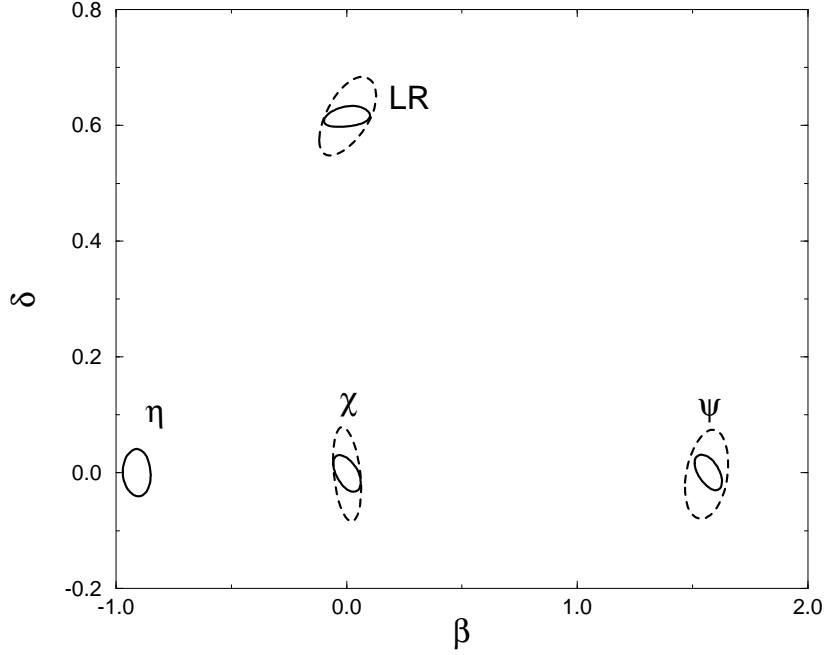


FIG. 2. 90% confidence level ($\Delta\chi^2 = 4.6$) contours (dashed lines) for β vs. δ for the typical models at the NLC. $M_{Z'} = 1$ TeV. The solid lines correspond to the assumption that the constraints $S_1 = S_2 = 0$ are satisfied. Only statistical error bars for the probes are used.

TABLE VI. Values and 1σ statistical error bars for S_2, β, δ for the typical models at the LHC. $S_1 = 0$ and $M_{Z'} = 1$ TeV. The error bars in parentheses are determined by setting $S_2 = 0$.

	χ	ψ	η	LR
S_2	0 ± 0.40	0 ± 0.16	0 ± 0.71	0 ± 0.54
β	$0 \pm 0.024(0.024)$	$1.57 \pm 0.028(0.028)$	$-0.912 \pm 0.010(0.010)$	$0 \pm 0.034(0.029)$
δ	$0 \pm 0.019(0.014)$	$0 \pm 0.022(0.016)$	$0 \pm 0.016(0.011)$	$0.615 \pm 0.021(0.004)$

B. Determination of the symmetry breaking structure at the LHC

At the LHC primarily three couplings (6) would be probed for a large class of models⁴. Namely, for $M_{Z'} = 1$ TeV and typical models specified in Table III $\gamma_q^\ell(P_L^q)$ cannot be determined with sufficient precision. Consequently, one can only determine the three combinations of S_2, β , and δ . We therefore set $S_1 = 0$, thus expressing the undetermined coupling P_L^q in terms of the three left-over couplings P_V^ℓ , P_R^u , and P_R^d . This constraint also removes one sign ambiguity (ϵ_q). Then, we fit for S_2, β , and δ . Thus, at the LHC one has to assume that one ($S_1 = 0$) of the two E_6 discrete constraints on the gauge couplings is already satisfied in order to further test whether or not the second discrete constraint $S_2 = 0$ is satisfied and then ultimately determine the values of β and δ .

In Table VI the values and expected 1σ uncertainties for these quantities are given for the models specified in Table III and $M_{Z'} = 1$ TeV. In general, there are eight disjoint regions corresponding to the different sign assignments for $\epsilon_u, \epsilon_d, \epsilon_\ell$. We only quote the results for the region in the vicinity of $S_2 = 0$.⁵ The parameters β and δ can be determined with uncertainties between 0.02 and 0.04 for a large class of typical models.

In Figure 3 we plot the 90% confidence level ($\Delta\chi^2 = 4.6$) contours (dashed lines) in the β vs. δ plane for the typical models specified in Table III with $M_{Z'} = 1$ TeV, and for the region in the vicinity of $S_2 = 0$.

⁴The LHC would also determine the Z' mass. It would furthermore establish whether there is a corresponding W' , as expected in LR models, and the ratio $M_{W'}/M_{Z'}$, which probes the LR -breaking mechanism [15].

⁵In general, the region in the vicinity of $S_2 = 0$ removes the few-fold sign ambiguity, thus uniquely fixing the value of β and δ . However, for special models, such a region can be fitted with more than one value of β and δ . *E.g.*, the couplings corresponding to the χ , and η models, can also be fitted to the models with $\delta = 0$, $\beta = \tan^{-1}(3\sqrt{3/5})$, and $\delta = 0$, $\beta = -\tan^{-1}(7\sqrt{3/5})$, respectively. The model with $\delta = 0$, $\beta = \tan^{-1}(\sqrt{3/5})$ is an alternative of the ψ model. In this case constraints $C_1 = C_2 = 0$ (or $S_1 = S_2 = 0$) are formally undetermined because they are obtained by dividing the first two constraints in (9) by $\hat{g}_L^\ell - \hat{g}_R^\ell = 0$. However, the first two constraints in (9) are satisfied. In Figure 3 we do not display any of the alternative regions.

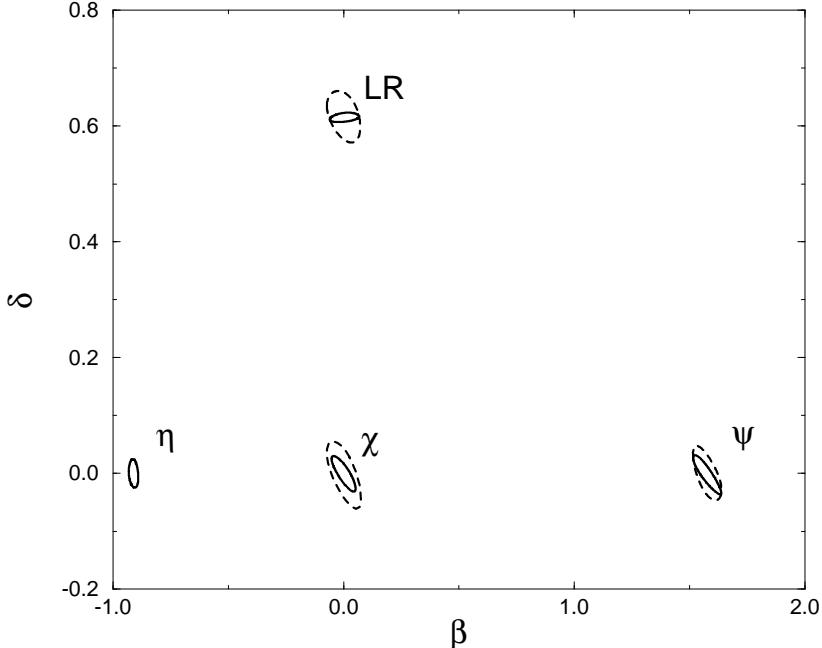


FIG. 3. 90% confidence level ($\Delta\chi^2 = 4.6$) contours for β vs. δ for the typical models at the LHC. $M_{Z'} = 1$ TeV. Only statistical error bars for the probes are used. Dashed lines are determined by fixing $S_1 = 0$, while the solid ones correspond to setting $S_2 = 0$ as well.

As a second step, we set S_2 to zero as well. In this case the fitted values for β and δ have smaller uncertainties. In Table VI the corresponding 1σ uncertainties are given in parentheses. The uncertainties are now reduced by a factor of 1 to 5 compared to the step one analysis. In Figure 3 the 90% confidence level ($\Delta\chi^2 = 4.6$) contours in β vs. δ are plotted with solid lines. The parameters can be determined with a precision of about a few percent. For the typical models the uncertainties are smaller than those at the NLC (see Figure 2).

Although the overall strength of the Z' gauge couplings does not enter in the above analysis (except for the estimate of typical statistical error), the overall strength of the interactions $g_2^2((\hat{g}_L^\ell)^2 + (\hat{g}_R^\ell)^2)$ can also be measured at the LHC, by measuring the cross-section in the main production channel and the total width. Determination of this coupling can be used to constrain further the symmetry breaking pattern [14].

V. CONCLUSIONS

We have demonstrated how the model independent determination of gauge couplings of a possible Z' at future colliders would allow one to gain information about the nature of the extended gauge structure associated with the Z' .

As a prime case we study E_6 [$SO(10)$] as the underlying gauge symmetry. In the case of E_6 [$SO(10)$] Z' gauge couplings have to satisfy two [three] discrete constraints. Provided such constraints are satisfied, the parameters $\tan\beta$ [$\beta = 0$ for $SO(10)$] and δ , which charac-

terize the effects of the symmetry pattern within $E_6 [SO(10)]$ on the Z' couplings, can be determined.

For $M_{Z'} \sim 1-2$ TeV and typical models the statistical uncertainties for parameters β and δ are in the 0.01–0.04 range, once the corresponding discrete constraints are fixed. We included only statistical uncertainties for the probes. Realistic fits, which include experimental cuts and detector acceptances, are expected to give larger uncertainties.

ACKNOWLEDGMENTS

The work was supported in part by CICYT under contract AEN94-0936 (F.del A.), the European Union under contract CHRX-CT92-0004 (F. del A.), the Junta de Andalucía (F. del A.) and the U.S. DOE Grant No. DOE-EY-76-02-3071 (M. C. and P.L.).

REFERENCES

- [1] F. del Aguila, M. Cvetič, and P. Langacker, Phys. Rev. **D48** (1993) R969 and references therein.
- [2] For a review, see M. Cvetič, F. del Aguila, and P. Langacker, in the Proceedings of the Workshop on *Physics and Experiments at Linear e^+e^- Colliders*, World Scientific (1993), F. Harris et al. eds., p. 929.
- [3] S. Godfrey, Carleton Univ. preprint, OCIP/C 94-4, hep-ph #9411237, Phys. Rev. **D51**, in press.
- [4] A. Djouadi, A. Leike, T. Riemann, D. Schaile and C. Verzegnassi, *Z. Phys.* **C56** (1992) 289; J. Hewett and T. Rizzo, in the Proceedings of the *Workshop on Physics and Experiments with Linear e^+e^- Colliders*, September 1991, Saariselkä, Finland, R. Orava ed., Vol. II, p. 489; *ibidem* p. 501.
- [5] F. del Aguila and M. Cvetič, Phys. Rev. **D50** (1994) 3158; A. Leike, *Z. Phys.* **C62** (1994) 265; see also D. Choudhury, F. Cuypers, and A. Leike, Phys. Lett. **B333** (1994) 531.
- [6] F. del Aguila, J.A. González, and M. Quirós, Phys. Lett. **B197** (1987) 89; Nucl. Phys. **B307** (1988) 571.
- [7] F. del Aguila, Acta Physica Polonica **B25** (1994) 1317.
- [8] F. del Aguila, M. Masip, and M. Pérez-Victoria, UG-FT-46/94; see F. del Aguila, G. Blair, M. Daniel, and G.G. Ross, Nucl. Phys. **B283** (1987) 50; F. del Aguila, M. Quirós, and F. Zwirner, Nucl. Phys. **B287** (1987) 419; F. del Aguila, G.D. Coughlan, and M. Quirós, Nucl. Phys. **B307** (1988) 633; (E) Nucl. Phys. **B312** (1989) 751 for early reference.
- [9] See for example, P. Langacker, hep-ph # 9412361, to be published in *Precision Tests of the Standard Electroweak Model*, ed. P. Langacker (World Scientific, Singapore 1995).
- [10] M. Cvetič, B. Kayser, and P. Langacker, Phys. Rev. Lett. **68** (1992) 2871.
- [11] P. Langacker and M. Luo, Phys. Rev. **D44** (1991) 817.
- [12] A. Henriques and L. Poggioli, ATLAS Collaboration, Note PHYS-NO-010 (October 1992); T. Rizzo, Phys. Rev. **D48** (1993) 4236.
- [13] P. K. Mohapatra, Mod. Phys. Lett. **A8** (1993) 771.
- [14] R. Robinett and J. Rosner, Phys. Rev. **D25** (1982) 3036, **D26** (1982) 2396; R. Robinett, Phys. Rev. **D26** (1982) 2388.
- [15] M. Cvetič, and P. Langacker, Phys. Rev. **D42** (1990) 1797.